Computer Methods in Applied Mechanics and Engineering 110 (1993) 343–357
North-Holland

A stable bilinear element for the Reissner–Mindlin plate model

Mikko Lyly, Rolf Stenberg and Teemu Vihinen
Faculty of Mechanical Engineering, Helsinki University of Technology, 02150 Espoo, Finland

Received 11 December 1992

In this paper, we introduce a new quadrilateral element using isoparametric bilinear basis functions for both components of the rotation vector and the deflection. The element is a stable modification of the MITC4 element. We report on calculations with this new element, the original MITC4 and also the bilinear element, with selective reduced integration. The numerical results are in accordance with the results of the numerical analysis and they show that (i) the method with reduced integration is highly unreliable and cannot be recommended; (ii) the MITC4 performs rather well, but its instability can lead to a decrease in accuracy for the deflection and especially to an inaccurate and oscillating shear force; (iii) the drawbacks of the MITC4 are not present in the modified method.

1. Introduction

The plate bending model by Reissner and Mindlin is today the dominating model used in finite element computations. This despite the fact that the elements have to be designed very carefully in order to avoid, or relax, the locking phenomena. The locking is most clearly seen in some low-order methods for which the finite element method will not bend at all when the plate is thin. It should be remembered, however, that similar phenomena will arise for many higher-order elements as well. For these, the locking may not be total, the finite element model will bend, but the accuracy is not as good as would be expected with the basis functions used.

Mathematically, the locking is the result of the lack of stability of the method. Another effect due to the nonstability of the method is that the calculated shear force can be oscillating and inaccurate. That this problem often occurs seems to be common knowledge (see the remark on p. 224 of [12]) but only recently has it been reported explicitly (cf. [16]).

During the last few years, significant progress has been made on the mathematical stability and error analysis of methods for Reissner–Mindlin plates. As a result, several new methods and families of methods have emerged, cf. [1, 3–5, 8, 12, 14, 19]. Of these the 'MITC' family [5] is one of the most attractive. The error analysis [4, 8] performed for these elements showed that they are optimally convergent for all elements which are of at least quadratic (triangles) or biquadratic (quadrilaterals) degree. The linear triangular element will not be convergent. For a restricted class of meshes, the bilinear MITC4 element was, however, shown [3, 4] to give an optimally convergent deflection and rotation, but the shear force will not be bounded in the L^2-norm, which would be the optimal estimate.

However, in the recent paper [8], it was shown that it is possible to obtain stable and optimally convergent linear and bilinear elements if one combines the 'covariant interpolation' technique of the MITC family with some recent stabilization techniques introduced in [12] and [19].

The purpose of this paper is to present the element obtained in this way from the bilinear MITC4 element. We give a computational assessment of this new element. We compare it with the original MITC4 and also to the 'classical' element with bilinear basis functions and a one-point reduced integration for the shear energy. Our aim has been to try to do as revealing computations as possible in

Correspondence to: Dr. R. Stenberg, Post code Y-OS, Faculty of Mechanical Engineering, Helsinki University of Technology, 02150 Espoo, Finland.

0045-7825/93/$06.00

order to detect possible shortcomings of the elements. In this, we have been guided by the theoretical results that have been derived for the elements.

In the next section we give the plate model and introduce our notation. In Section 3, we first recall the MITC4 element and then we introduce our stabilized modification of it. We also recall the formulation of the element with selective reduced integration. In this section, we collect the theoretical results that are known for these methods. In Section 4 we give the results of our numerical calculations. Conclusions are presented in Section 5.

2. The plate bending problem considered

Let Ω be the bounded two-dimensional region occupied by the plate. The unknowns of the problem are the deflection $w(x, y)$ and the rotation vector $\boldsymbol{\beta}(x, y) = (\beta_x, \beta_y)$. They are determined from the condition that they minimize the energy of the plate:

$$E(w, \boldsymbol{\beta}) = \min_{(v, \boldsymbol{\psi}) \in \mathcal{U}_{\mathrm{ad}}} E(v, \boldsymbol{\psi}) , \tag{2.1}$$

with the energy defined as

$$E(v, \boldsymbol{\psi}) = \frac{1}{2} t^3 a(\boldsymbol{\psi}, \boldsymbol{\psi}) + \frac{1}{2} G\kappa t \int_\Omega |\boldsymbol{\psi} - \nabla v|^2 \, \mathrm{d}\Omega - \int_\Omega g v \, \mathrm{d}\Omega . \tag{2.2}$$

Here $\mathcal{U}_{\mathrm{ad}}$ denotes the collection of kinematically admissible pairs of deflections and rotations for which the strain energy is finite. We assume that the boundary conditions are such that the solution is unique. g is the applied transversal load and t denotes the thickness of the plate. G is the shear modulus and κ is the shear correction factor commonly used in this context. The first term on the right-hand side of (2.2) represents the bending energy with the bilinear form defined as

$$a(\boldsymbol{\beta}, \boldsymbol{\psi}) = \frac{E}{12(1 - \nu^2)} \int_\Omega [(1 - \nu)\boldsymbol{\varepsilon}(\boldsymbol{\beta}) : \boldsymbol{\varepsilon}(\boldsymbol{\psi}) + \nu \operatorname{div} \boldsymbol{\beta} \operatorname{div} \boldsymbol{\psi}] \, \mathrm{d}\Omega . \tag{2.3}$$

Here E and ν denote Young's modulus and the Poisson ratio, respectively. $\boldsymbol{\varepsilon}(\cdot)$ is the linear strain operator and 'div' stands for the divergence, viz.

$$\boldsymbol{\varepsilon}(\boldsymbol{\beta}) = \frac{1}{2} \{\nabla \boldsymbol{\beta} + (\nabla \boldsymbol{\beta})^{\mathrm{t}}\} , \tag{2.4}$$

$$\operatorname{div} \boldsymbol{\beta} = \frac{\partial \beta_x}{\partial x} + \frac{\partial \beta_y}{\partial y} . \tag{2.5}$$

For two symmetric second order tensors $\boldsymbol{\sigma}$ and $\boldsymbol{\gamma}$ we define

$$\boldsymbol{\sigma} : \boldsymbol{\gamma} = \sigma_x \gamma_x + 2\sigma_{xy}\gamma_{xy} + \sigma_y \gamma_y . \tag{2.6}$$

Let us also recall that from the solution $(w, \boldsymbol{\beta})$, the bending moment $\boldsymbol{M}$ and the shear force $\boldsymbol{Q}$ are obtained from

$$\boldsymbol{M} = -\frac{Et^3}{12(1 - \nu^2)} \{(1 - \nu)\boldsymbol{\varepsilon}(\boldsymbol{\beta}) + \nu \operatorname{div} \boldsymbol{\beta} \boldsymbol{I}\} , \tag{2.7}$$

where $\boldsymbol{I}$ denotes the indentity tensor, and

$$\boldsymbol{Q} = G\kappa t(\boldsymbol{\beta} - \nabla w) . \tag{2.8}$$

The possible 'locking' of a finite element model will appear for a 'thin' plate and in order to make a rigorous analysis of this, it is customary (cf. [7, 12]) to consider the sequence of problems where the loading is given by

$$g = t^3 f\,, \tag{2.9}$$

with f fixed independent of the thickness t. By this, it is ensured that the problem has a finite non-vanishing solution in the limit $t \to 0$. In this limit, the Kirchhoff condition

$$\boldsymbol{\beta} = \nabla w \tag{2.10}$$

will be valid and the locking is due to a too strong enforcement of it in the finite element model. In an analysis, it is also appropriate to consider the scaled shear force $\boldsymbol{q} = t^{-3}\boldsymbol{Q}$, i.e.

$$\boldsymbol{q} = G\kappa t^{-2}(\boldsymbol{\beta} - \nabla w)\,. \tag{2.11}$$

The solution to the Reissner–Mindlin equations exhibits a boundary layer (cf. [2] for a survey) and hence the solution will usually not be very smooth even if the loading and the boundary are smooth. However, some regularity estimates can be proved (cf. [1, 7]) and these are used in Theorems 3.1 and 3.3 in order to present the estimates in a simple form.

3. The finite element methods

Our new element, the MITC4 and the method with selective reduced integration, all utilize isoparametric bilinear basis functions for the deflection and both components of the rotation. Hence we have

$$\mathcal{U}_{\mathrm{ad}}^h = \{(v, \boldsymbol{\psi}) \in \mathcal{U}_{\mathrm{ad}} \,|\, (v, \boldsymbol{\psi})|_K \in [Q_1(K)]^3 \;\forall K \in \mathcal{C}_h\}\,. \tag{3.1}$$

Here $\mathcal{C}_h$ denotes the partitioning of the domain into convex quadrilaterals and $Q_1(K)$ denotes the space of isoparametric bilinear functions on K (cf. [11]). Henceforth we assume that the domain is polygonal.

The finite element methods are then defined as follows: Find $(w_h, \boldsymbol{\beta}_h) \in \mathcal{U}_{\mathrm{ad}}^h$ satisfying

$$E_h(w_h, \boldsymbol{\beta}_h) = \min_{(v,\boldsymbol{\psi}) \in \mathcal{U}_{\mathrm{ad}}^h} E_h(v, \boldsymbol{\psi})\,, \tag{3.2}$$

with the discrete energy E_h defined differently for the three methods.

Let us first recall the element introduced by Bathe and Dvorkin.

3.1. The MITC4 element [6]

For any $K \in \mathcal{C}_h$, let $\boldsymbol{F}_K = (F_{x,K}, F_{y,K})$ be the bilinear mapping of the unit square $\hat{K}$ onto K. The Jacobian matrix of $\boldsymbol{F}_K$, we denote by $\boldsymbol{J}_K$, i.e.

$$\boldsymbol{J}_K = \begin{bmatrix} \dfrac{\partial F_{x,K}}{\partial \xi} & \dfrac{\partial F_{x,K}}{\partial \eta} \\[2ex] \dfrac{\partial F_{y,K}}{\partial \xi} & \dfrac{\partial F_{y,K}}{\partial \eta} \end{bmatrix}, \tag{3.3}$$

where (ξ, η) are the coordinates of $\hat{K}$ (i.e. the natural coordinates of K). We remark here that in the finite element literature, the name Jacobian is often used for the transpose of the above matrix. We will, however, use the more established definition. Further, let

$$\boldsymbol{\Gamma}(\hat{K}) = \{\hat{s} = (\hat{\gamma}_\xi, \hat{\gamma}_\eta) \mid \hat{\gamma}_\xi = a + b\eta,\ \hat{\gamma}_\eta = c + d\xi, \text{ for some } a, b, c, d \in \mathbb{R}\} \tag{3.4}$$

and

$$\boldsymbol{\Gamma}(K) = \{s = (\gamma_x, \gamma_y) \mid s(x, y) = \boldsymbol{J}_K^{-t}\hat{s}(\boldsymbol{F}_K^{-1}(x, y)) \text{ for some } \hat{s} \in \boldsymbol{\Gamma}(\hat{K})\}\ , \tag{3.5}$$

with $\boldsymbol{J}_K^{-t}$ denoting the transpose of $\boldsymbol{J}_K^{-1}$. For a given vector valued function s, the reduction operator $\boldsymbol{R}_h$ is defined so that $\boldsymbol{R}_h s \mid_K \in \boldsymbol{\Gamma}(K)$ and determined through

$$\int_E [(\boldsymbol{R}_h s - s)\cdot \boldsymbol{\tau}]\, ds = 0 \quad \text{for every edge } E \text{ of } K, \text{ for each } K \in \mathscr{C}_h\ . \tag{3.6}$$

Here $\boldsymbol{\tau}$ is the tangent to the edge E.

The method is now defined from (3.2) with

$$E_h(v, \boldsymbol{\psi}) = \frac{1}{2}t^3 a(\boldsymbol{\psi}, \boldsymbol{\psi}) + \frac{1}{2}G\kappa t\int_\Omega |\boldsymbol{R}_h\boldsymbol{\psi} - \nabla v|^2\, d\Omega - \int_\Omega gv\, d\Omega \tag{3.7}$$

for all v in the finite element subspace for the deflection.

The approximation for the shear force is obtained from

$$\boldsymbol{Q}_h = G\kappa t(\boldsymbol{R}_h\boldsymbol{\beta}_h - \nabla w_h)\ . \tag{3.8}$$

REMARK 1. We point out that for a function v in the finite element subspace for the deflection, $\nabla v|_K = \boldsymbol{J}_K^{-t}\hat{\nabla}\hat{v}|_K$ holds for all $K \in \mathscr{C}_h$, with $\hat{v}(\xi, \eta)|_K = v(F_{x,K}(\xi, \eta), F_{y,K}(\xi, \eta))|_K$ and $\hat{\nabla}$ denoting the gradient with respect to the (ξ, η) variables. Since $\hat{\nabla}\hat{v}(\xi, \eta)|_K \in \boldsymbol{\Gamma}(\hat{K})$, it follows that $\boldsymbol{R}_h\nabla v = \nabla v$.

REMARK 2. In [6], the reduction operator $\boldsymbol{R}_h$ is defined using a different notation. By using some tensor analysis (cf. e.g. [10, 21]) it is easily seen that the above definition is identical to that of [6].

REMARK 3. For a rectangular element, the MITC4 coincides with the T1 element of Tezduyar and Hughes [13] and the QUAD4 element of MacNeal [17].

In [3], it was shown that this element is closely related to the so-called 'Q_1–P_0' element for the Stokes problem and that the error estimates known for that (cf. [20]) can be transferred to the present element. In [3, 4], this was done for the case of rectangular elements, but it can be extended [22] to the same class of elements for which the Stokes element has been analyzed. This class is given as follows.

ASSUMPTION MI. Let $\mathscr{C}_{4h}$ be a partitioning of $\bar{\Omega}$ into regular quadrilaterals. Divide the unit square $\hat{K}$ into 4×4 equal squares $\hat{K}_{ij}$, $i, j = 1, 2, 3, 4$, and let $\boldsymbol{F}_M$ be the bilinear mapping of $\hat{K}$ onto the 'macroelement' $M \in \mathscr{C}_{4h}$. The mesh $\mathscr{C}_h$ is then defined by (cf. Fig. 1) $\mathscr{C}_h = \{K \mid K = \boldsymbol{F}_M(\hat{K}_{ij}),\ M \in \mathscr{C}_{4h},\ i, j = 1, 2, 3, 4\}$.

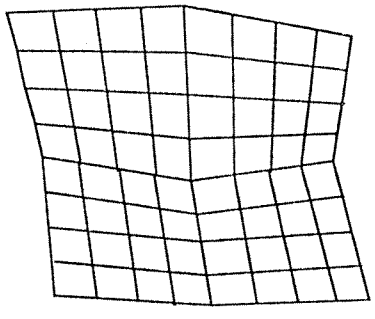

Fig. 1. Example of a mesh constructed so that Assumption MI holds.

For both the MITC4 and its stabilized modification, we need one additional assumption on the mesh. This in order that the operator $\boldsymbol{R}_h$ has the optimal approximation property (cf. [25]).

ASSUMPTION MII. For an element $K \in \mathscr{C}_h$ let δ_K denote the distance between the midpoints of the two diagonals of K. We then assume that $\delta_K \leq Ch_K^2$ for every $K \in \mathscr{C}_h$.

For simplicity, we present the error estimates for the MITC4 and its modification for the case of a clamped plate and a convex domain. For this case, the solution is regular enough in order that the methods will converge with the optimal order, and the estimates can be concisely stated by using the L^2-norm of the load. For a more general case, one would need to give the estimate with the help of the regularity of the exact solution (cf. [8]).

We use standard Sobolev space notation (cf. [11, Appendix 4I]). As usual, h denotes the mesh parameter. By C we denote various positive constants independent of the mesh parameter h and the plate thickness t. This means that under the assumptions stated in the theorems, the three finite element methods below will not show any locking of the deflection.

THEOREM 3.1 [3, 4, 22]. Suppose that the mesh $\mathscr{C}_h$ satisfies Assumptions MI and MII. Suppose further that the plate is clamped and that Ω is convex. For $f \in L^2(\Omega)$, it then holds that

$$\|w - w_h\|_1 + \|\boldsymbol{\beta} - \boldsymbol{\beta}_h\|_1 \leq Ch\|f\|_0 . \tag{3.9}$$

REMARK 4. If one imposes the additional assumption that the elements are rectangular, then the following L^2-estimate holds [3, 4]:

$$\|w - w_h\|_0 \leq Ch^2\|f\|_0 . \tag{3.10}$$

REMARK 5. For the Q_1–P_0 Stokes element, the pressure is not convergent in general (cf. [20]). This means that for the MITC4, we cannot assure that the L^2-error for the shear is bounded independent of t. For the case of rectangular elements and a quasi-uniform mesh (i.e. $h \leq Ch_K$, for all $K \in \mathscr{C}_h$), the analysis of [20] and [15] would give the estimate

$$\|\boldsymbol{q} - \boldsymbol{q}_h\|_0 \leq C\left(\frac{h}{t + h^2}\right)\|f\|_0 , \tag{3.11}$$

which shows that the error in the shear is very sensitive to the plate thickness. Here and below we denote $\boldsymbol{q}_h = t^{-3}\boldsymbol{Q}_h$ where $\boldsymbol{Q}_h$ is the approximate shear force of the method in question.

Let us also recall that for the Q_1–P_0 element, it is known (for meshes satisfying MII) how to filter the pressure in order to get a convergent pressure. We do not know, however, how this filtering could be carried over to the MITC4.

In view of the above theorem and remarks, it seems that the following method is both simpler and more robust than the MITC4.

3.2. The new stabilized form of MITC4

We now modify the method by defining the discrete energy as

$$E_h(v, \boldsymbol{\psi}) = \frac{t^3}{2}a(\boldsymbol{\psi}, \boldsymbol{\psi}) + \sum_{K \in \mathscr{C}_h} \frac{G\kappa t^3}{2(t^2 + \alpha h_K^2)} \int_K |\boldsymbol{R}_h\boldsymbol{\psi} - \nabla v|^2 \, d\Omega - \int_\Omega gv \, d\Omega . \tag{3.12}$$

Here h_K denotes the longest of the edges of the element $K \in \mathscr{C}_h$. α is a fixed positive constant. The reduction operator is defined as for the original MITC4. The approximate shear force is obtained from

$$\boldsymbol{Q}_{h|K} = \frac{G\kappa t^3}{(t^2 + \alpha h_K^2)} (\boldsymbol{R}_h \boldsymbol{\beta}_h - \nabla w_h)_{|K} \quad \text{for each element } K \in \mathscr{C}_h . \tag{3.13}$$

The above stabilization technique was first introduced in [19] (cf. also [12]) but there it was required that the deflection is piecewise quadratic. In [8], it was shown that one can use linear or bilinear elements for the deflection if one includes an MITC reduction operator. We did the analysis for the case of linear elements and with the local mesh length h_K was replaced by the global mesh parameter h, but it is possible to perform the analysis for the above formulation as well. This will be done in a forthcoming paper [22]. One can prove optimal error estimates for a general mesh (i.e. regular in the usual sense, cf. [11]).

THEOREM 3.2. [8, 23]. Suppose that the plate is clamped, that Ω is convex and that the mesh $\mathscr{C}_h$ satisfies Assumption MII. With $f \in L^2(\Omega)$, it then holds that

$$\|w - w_h\|_1 + \|\boldsymbol{\beta} - \boldsymbol{\beta}_h\|_1 + \left(\sum_{K \in \mathscr{C}_h} h_K^2 \|\boldsymbol{q} - \boldsymbol{q}_h\|_{0,K}^2 \right)^{1/2} + t\|\boldsymbol{q} - \boldsymbol{q}_h\|_0 \leq Ch\|f\|_0 . \tag{3.14}$$

REMARK 6. For a quasi-uniform mesh, this gives

$$\|\boldsymbol{q} - \boldsymbol{q}_h\|_0 \leq C\left(\frac{h}{t+h}\right)\|f\|_0 \tag{3.15}$$

for the shear. Hence, we see that the shear does not necessarily have to converge but it stays bounded independent of the plate thickness. We recall that this does not have to be the case for the original MITC4.

Let us also point out that the above modification has the advantage that the stiffness matrix is more well conditioned which will be of importance, e.g. when some iterative solution method is considered; cf. [18] where this observation is used for designing multigrid methods.

3.3. *The element with selective reduced integration*

In this element we minimize

$$E_h(v, \boldsymbol{\psi}) = \frac{1}{2} t^3 a(\boldsymbol{\psi}, \boldsymbol{\psi}) + \frac{1}{2} G\kappa t \int_\Omega |\boldsymbol{R}_h(\boldsymbol{\psi} - \nabla v)|^2 \, \mathrm{d}\Omega - \int_\Omega gv \, \mathrm{d}\Omega \tag{3.16}$$

with the reduction operator $\boldsymbol{R}_h$ defined from

$$(\boldsymbol{R}_h \boldsymbol{\phi})|_K = \text{value of } \boldsymbol{\phi} \text{ at the midpoint of the element } K \text{ for every } K \in \mathscr{C}_h . \tag{3.17}$$

This is usually stated as a 'selective reduced integration': the bending energy is integrated exactly whereas the one point Gauss rule is used for the shear term. The approximate shear force is piecewise constant calculated from

$$\boldsymbol{Q}_h = G\kappa t \boldsymbol{R}_h(\boldsymbol{\beta}_h - \nabla w_h) . \tag{3.18}$$

This method was one of the first that was shown to give satisfactory results for thin plates. However, it is easily seen that the method cannot be stable; if we consider the case of a completely free plate, the solution to the finite element model will exhibit unphysical 'zero energy modes' (cf. e.g., [11, pp. 332–335]). With enough enforced boundary conditions, these zero energy modes will be eliminated, but they are a sign of the instability of the method and this can often cause some problems.

In spite of its known deficiencies, this element is presented in most modern textbooks such as [9, 11].

Although the method is not stable, it has been possible to prove error estimates in some particular cases; cf. [15] by Johnson and Pitkäranta. They consider the clamped plate and rectangular elements and the estimate they prove is as follows.

THEOREM 3.3 [15]. Let the plate be clamped and suppose that Ω is a rectangle with a partitioning $\mathscr{C}_h$ consisting of equal rectangular elements. If $w \in H^5(\Omega)$, $\boldsymbol{\beta} \in [H^4(\Omega)]^2$ and $\boldsymbol{q} \in [H^1(\Omega)]^2$, we then have

$$\|w - w_h\|_1 + \|\boldsymbol{\beta} - \boldsymbol{\beta}_h\|_1 + (t + h^3)\|\boldsymbol{q} - \boldsymbol{q}_h\|_0 \leq Ch(\|w\|_5 + \|\boldsymbol{\beta}\|_4 + \|\boldsymbol{q}\|_1) . \tag{3.19}$$

REMARK 7. In [15] the following estimate is also reported:

$$\|w - w_h\|_0 \leq Ch^{3/2}(\|w\|_5 + \|\boldsymbol{\beta}\|_4 + \|\boldsymbol{q}\|_1) . \tag{3.20}$$

We first note that compared to the estimates for the two previous methods, here we need more regularity of the exact solution (and the load). Furthermore, the proof given in [15] relies heavily on the assumptions of rectangular elements and clamped boundary conditions and substantial generalizations seem hard to obtain. Let us also remark that for some of the discrete shear components, the estimate derived is better, but the 'filtering' operator needed to improve the shear would be quite complicated, and for a nonrectangular mesh unknown.

The analysis in [15] is based on the equivalence between the present element and a mixed method with piecewise constant approximations for the shear. For a general quadrilateral, this equivalence does not hold. Hence, in our calculations we could have considered the mixed method, but we chose the present method since this is the method usually presented in the literature [9, 11].

4. Numerical experiments

We perform all our numerical experiments for a clamped square plate with a uniformly distributed load. We show that it is possible to obtain quite revealing results with this seemingly simple problem. In the calculations, we have chosen the Poisson ratio $\nu = 0.3$ and the shear correction factor $\kappa = 5/6$. The side length of the square is chosen equal to unity. Due to the symmetry, only one-fourth of the square is discretized and hence the side of the computational domain is 0.5. We consider the case of a 'thin' plate. The solution to the problem is then very near the Kirchhoff solution obtained in the limit when $t \to 0$. For the Kirchhoff plate, an exact solution is easily computed by classical means. Hence, that is considered as the exact solution.

Below we perform several tests where we check the accuracy and sensitivity of the methods with respect to distortions of the mesh and changes in the thickness of the plate.

In the stabilized MITC4, we have chosen $\alpha = 0.1$ and as the parameter h_K we take the length of the longest side of the element K. In our last numerical test, we study how the accuracy of the stabilized MITC4 depends on the parameter α.

4.1. Results for uniform and randomly distorted meshes

In our first test, we choose $t = 0.01$. We consider a finite element partitioning into $N \times N$ equal squares (see Fig. 2).

The calculations are then repeated with a sequence of distorted meshes. These are constructed from the regular ones by moving each interior node at random within a square centered at the node and with side length $0.4h$ where h $(=1/N)$ is the side length of the original elements. The nodes lying on the sides of the computational domain are moved in the same way in the direction of the sides. The meshes obtained are presented in Fig. 3.

Below we give the results of our calculations. From Table 1 we see that for the MITC4 and its stabilized modification (abbreviated as 'STAB'), the mesh distortion will not affect the accuracy of the centerpoint deflection except for the coarsest mesh. For the method with selective reduced integration

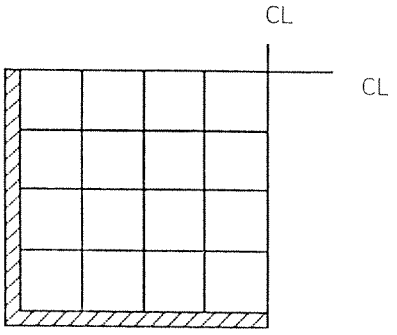

Fig. 2. The uniform mesh for $N = 4$.

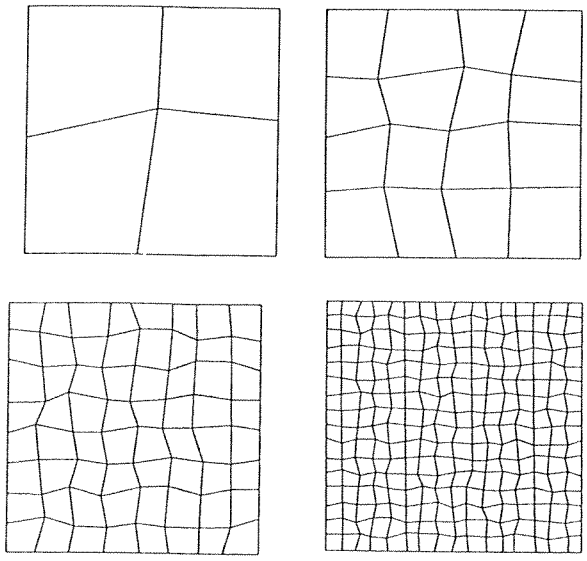

Fig. 3. The distorted meshes.

Table 1
The normalized centerpoint deflections w_h(center)/w(center) for the uniform and distorted meshes for $t = 0.01$

	Selective reduced integration		MITC4		Stabilized MITC4	
N	Uniform	Distorted	Uniform	Distorted	Uniform	Distorted
2	0.9593	0.9648	0.9590	0.9177	1.0673	1.1602
4	0.9905	0.8862	0.9904	0.9915	1.0205	1.0252
8	0.9991	0.9151	0.9991	0.9964	1.0068	1.0062
16	1.0013	0.9804	1.0013	1.0008	1.0032	1.0032

(abbreviated as 'SRI'), however, the accuracy is decreased (that this does not happen for the coarsest mesh seems to be a coincidence, cf. Section 4.3).

That the mesh distortion seriously affects the accuracy of the deflection for the SRI is even more clearly seen from Table 2; for $N = 4$ the distortion increases the L^2-error by double and for $N = 16$ the increase in the error is about tenfold. This can be expected from the theoretical analysis; as already mentioned, the analysis of [15] is based heavily on the assumption of rectangular elements (for the uniform case we see that the accuracy is better than predicted by the estimate (3.23)). The distortion has no significant influence on the error for the MITC4 and STAB. For reference, we have also listed the error for the normal Lagrange interpolant in the finite element space for the deflection. We see that with respect to this error measure the stabilized method is better than both the SRI and the MITC4, and also slightly better than the interpolant.

Next, we give the errors in the moments and also for the moment obtained from the bilinear interpolant of the rotation (i.e. calculated from (2.7) with $\boldsymbol{\beta}$ replaced by its Lagrange interpolant)

Table 2
The errors $\|w - w_h\|_0 / \|w\|_0$ for the uniform and distorted meshes for $t = 0.01$

	Selective reduced integration		MITC4		Stabilized MITC4		Interpolant	
N	Uniform	Distorted	Uniform	Distorted	Uniform	Distorted	Uniform	Distorted
2	0.2687	0.2462	0.2691	0.2876	0.1539	0.1192	0.1504	0.1443
4	0.0698	0.1448	0.0699	0.0773	0.0408	0.0436	0.0474	0.0542
8	0.0161	0.0925	0.0161	0.0203	0.0095	0.0109	0.0126	0.0134
16	0.0027	0.0251	0.0027	0.0033	0.0025	0.0027	0.0032	0.0034

Table 3
The errors $\|\boldsymbol{M} - \boldsymbol{M}_h\|_0 / \|\boldsymbol{M}\|_0$ for the uniform and distorted meshes for $t = 0.01$

	Selective reduced integration		MITC4		Stabilized MITC4		Interpolant	
N	Uniform	Distorted	Uniform	Distorted	Uniform	Distorted	Uniform	Distorted
2	0.6057	0.6320	0.6058	0.6265	0.6035	0.6397	0.6055	0.6294
4	0.3187	0.3688	0.3187	0.3464	0.3182	0.3429	0.3188	0.3419
8	0.1613	0.2217	0.1613	0.1714	0.1612	0.1680	0.1613	0.1672
16	0.0809	0.1065	0.0809	0.0849	0.0809	0.0844	0.0809	0.0840

(Table 3). Here the mesh distortion has a quite small effect on any of the methods (although the biggest change is again for the SRI).

The effect of the mesh distortion is most pronounced for the shear force as could be expected from the theoretical analysis. From Table 4 we see that for the uniform mesh all three methods give a shear which is much better than predicted by the theory. This convergence of the shear is probably due to some superconvergence effects. By distorting the mesh, however, the instabilities surface; the accuracy of the shear for the SRI is completely destroyed and for coarser meshes the accuracy for the MITC4 is also affected. For finer meshes, the MITC4 starts to catch up with the stabilized method. The conclusion is, however, that the stabilized method is far more reliable than the other two. In Fig. 4 we show the distribution of the calculated shear forces along the horizontal symmetry line of the plate (along which the exact solution satisfies $Q_y = 0$). The graphs are for the distorted meshes with $N = 16$. Here we see how irregular and oscillating the shear is for the SRI. The stabilized method gives better results than the original MITC4, but for this mesh and value of t, the difference is not as big as it is for coarser meshes or smaller values of the thickness (cf. below). Let us also note that even if Assumption MII is not valid for the randomly distorted meshes, only the accuracy of the shear force is affected.

The next test is to repeat all calculations for a very thin plate with $t = 0.001$. The results are listed in Tables 5–8.

Again, we see that all three methods work very well as long as the mesh is uniform. For the distorted mesh, the situation is different. Now the SRI fails completely and the moment is very bad. For the coarsest mesh with $N = 2$, the MITC4 locks totally. The L^2-error of the deflection in the MITC4 is also affected for all meshes. Furthermore, for this thickness, the shear is very bad. In Fig. 5, we show the shear distribution for the MITC4 and the stabilized method for the distorted meshes with $N = 8$. We point out that the vertical scale is different here from that of Fig. 4 (the shear for the SRI is so highly oscillating that there is no point in showing it).

4.2. *Results for meshes obtained by moving one node*

Next we show that the instabilities in the SRI and MITC4 can show up in a quite innocent looking test; we only move one vertex in the mesh (see Fig. 6). Here we have moved the node which is nearest the clamped corner. This has a big effect on the MITC4. Results obtained by moving a node in the middle of the domain are presented in [23].

From Tables 9 and 10 we see that this can have a very dramatic effect on the shear force. This distortion does not have any effect on the moment for any of the three methods. For the thinner case of $t = 0.001$, the accuracy of the deflection will also be affected as can be seen from Table 11. Note that for $N = 4$, the effect on the deflection of the MITC4 is bigger than for the randomly distorted meshes.

Table 4
The errors $\|\boldsymbol{Q} - \boldsymbol{Q}_h\|_0 / \|\boldsymbol{Q}\|_0$ for the uniform and distorted meshes for $t = 0.01$

	Selective reduced integration		MITC4		Stabilized MITC4	
N	Uniform	Distorted	Uniform	Distorted	Uniform	Distorted
2	0.5199	2.7209	0.4530	5.5407	0.4413	0.4579
4	0.2546	3.9164	0.2772	0.6834	0.2757	0.3137
8	0.1328	3.9063	0.1761	0.5660	0.1760	0.2783
16	0.0784	2.4186	0.1172	0.2652	0.1174	0.1919

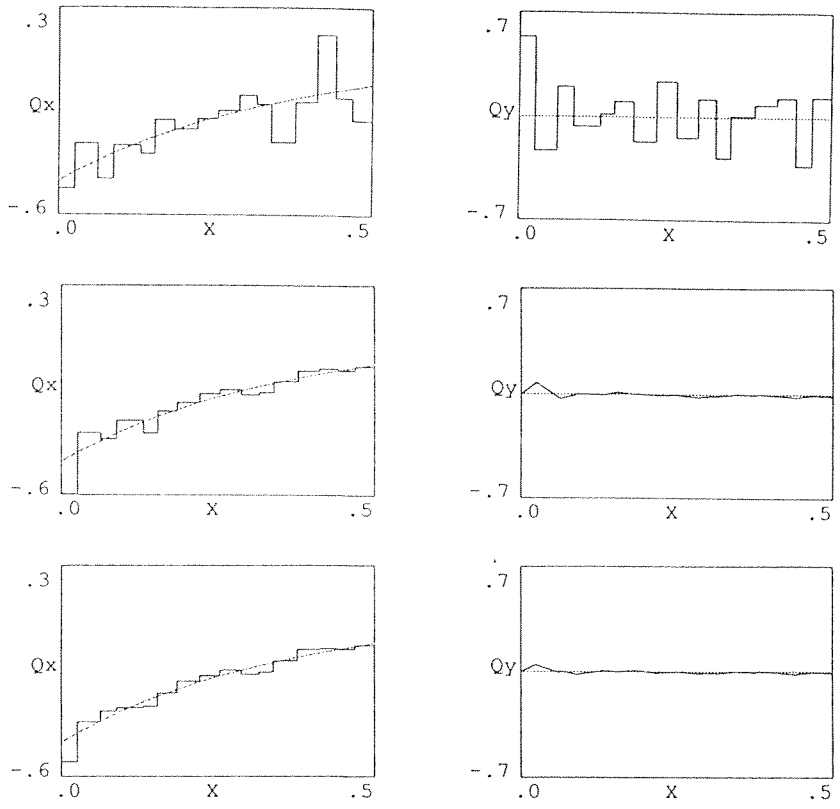

Fig. 4. The shear force distribution along the horizontal symmetry line for the method with selective reduced integration (top), MITC4 (middle) and stabilized MITC4 (bottom). A distorted mesh with $N = 16$. The thickness of the plate is $t = 0.01$. The dotted lines give the exact solution.

Table 5
The normalized centerpoint deflections w_h(center)/w(center) for the uniform and distorted meshes for $t = 0.001$

	Selective reduced integration		MITC4		Stabilized MITC4	
N	Uniform	Distorted	Uniform	Distorted	Uniform	Distorted
2	0.9573	0.2685	0.9573	0.0720	1.0656	1.1585
4	0.9885	0.3835	0.9885	1.0019	1.0186	1.0233
8	0.9971	0.6329	0.9971	0.9942	1.0048	1.0041
16	0.9993	0.8114	0.9993	0.9982	1.0012	1.0011

Table 6
The errors $\|w - w_h\|_0 / \|w\|_0$ for the uniform and distorted meshes for $t = 0.001$

	Selective reduced integration		MITC4		Stabilized MITC4		Interpolant	
N	Uniform	Distorted	Uniform	Distorted	Uniform	Distorted	Uniform	Distorted
2	0.2711	0.7859	0.2712	0.9432	0.1554	0.1191	0.1504	0.1443
4	0.0720	0.5134	0.0720	0.0840	0.0422	0.0447	0.0474	0.0542
8	0.0183	0.3385	0.0183	0.0261	0.0107	0.0122	0.0126	0.0134
16	0.0046	0.2070	0.0046	0.0063	0.0027	0.0031	0.0032	0.0034

4.3. *A study of the distortion robustness for a coarse mesh*

Next, we perform a test introduced by Weissman and Taylor [24]. We take the uniform 2×2 mesh and move the center node along one of the meshlines (cf. Fig. 7).

Table 7
The errors $\|\boldsymbol{M}-\boldsymbol{M}_h\|_0/\|\boldsymbol{M}\|_0$ for the uniform and distorted meshes for $t=0.001$

	Selective reduced integration		MITC4		Stabilized MITC4		Interpolant	
N	Uniform	Distorted	Uniform	Distorted	Uniform	Distorted	Uniform	Distorted
2	0.6059	0.8207	0.6059	0.9503	0.6035	0.6397	0.6055	0.6294
4	0.3188	0.6892	0.3188	0.3554	0.3182	0.3430	0.3188	0.3419
8	0.1613	0.5399	0.1613	0.1839	0.1612	0.1683	0.1613	0.1672
16	0.0809	0.4176	0.0809	0.0919	0.0809	0.0847	0.0809	0.0840

Table 8
The errors $\|\boldsymbol{Q}-\boldsymbol{Q}_h\|_0/\|\boldsymbol{Q}\|_0$ for the uniform and distorted meshes for $t=0.001$

	Selective reduced integration		MITC4		Stabilized MITC4	
N	Uniform	Distorted	Uniform	Distorted	Uniform	Distorted
2	0.5216	74.0530	0.4533	43.2862	0.4414	0.4585
4	0.2552	29.4427	0.2774	3.7011	0.2758	0.3162
8	0.1282	21.6957	0.1762	3.8323	0.1760	0.3011
16	0.0644	30.1994	0.1172	2.5511	0.1172	0.2723

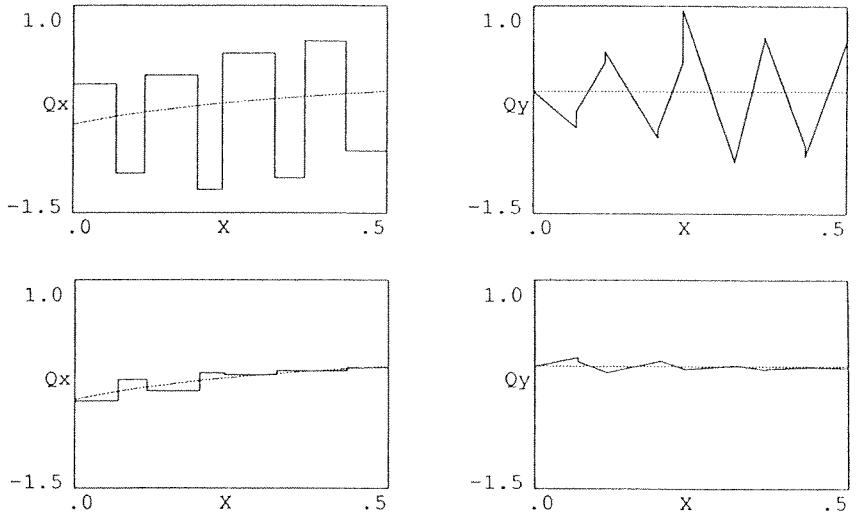

Fig. 5. The shear force distribution along the horizontal symmetry line for the MITC4 (top) and the stabilized MITC4 (bottom). A distorted mesh with $N=8$. Plate thickness $t=0.001$. The dotted lines give the exact solution.

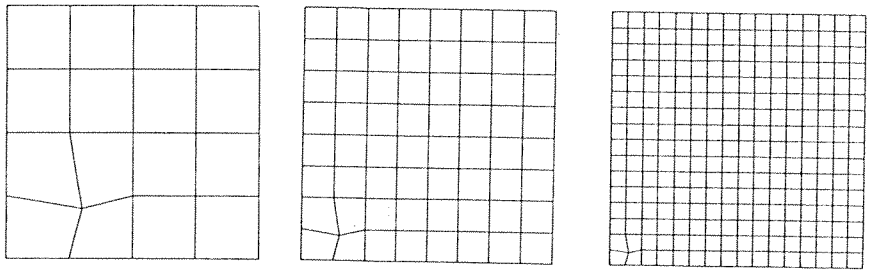

Fig. 6. The meshes obtained from the uniform ones by moving one node.

Table 9
The errors $\|\boldsymbol{Q}-\boldsymbol{Q}_h\|_0/\|\boldsymbol{Q}\|_0$ for a mesh obtained by moving one node in the uniform partitioning, $t=0.01$

N	Selective reduced integration	MITC4	Stabilized MITC4
4	1.5283	1.4494	0.3171
8	0.2280	0.2341	0.1846
16	0.0795	0.1186	0.1180

Table 10
The errors $\|\boldsymbol{Q}-\boldsymbol{Q}_h\|_0/\|\boldsymbol{Q}\|_0$ for a mesh obtained by moving one node in the uniform partitioning, $t=0.001$

N	Selective reduced integration	MITC4	Stabilized MITC4
4	20.6448	20.8639	0.3203
8	5.2072	5.1977	0.1874
16	0.6435	0.2928	0.1187

Table 11
The errors $\|w-w_h\|_0/\|w\|_0$ for a mesh obtained by moving one node in the uniform partitioning, $t=0.001$

N	Selective reduced integration	MITC4	Stabilized MITC4
4	0.1511	0.1513	0.0438
8	0.0196	0.0191	0.0108
16	0.0046	0.0046	0.0027

In Figs. 8–11, we see how the errors for the three methods vary with the distance δ by which the node is moved. From the figures we see that the stabilized method is much more robust than the two others. The shear force is again the quantity where difference is biggest; the SRI and the MITC4 both fail completely except for the uniform mesh.

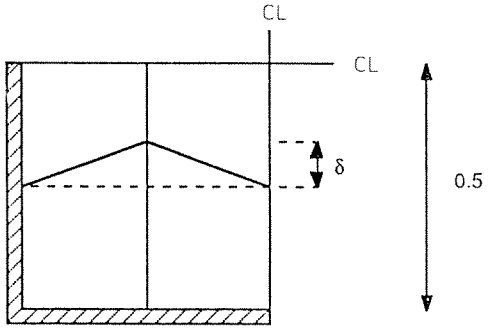

Fig. 7. The distortion of the 2×2 mesh.

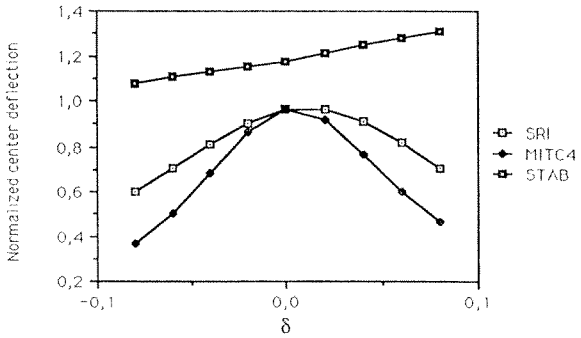

Fig. 8. The distortion sensitivity of the errors w_h(center)/w(center) for the 2×2 mesh.

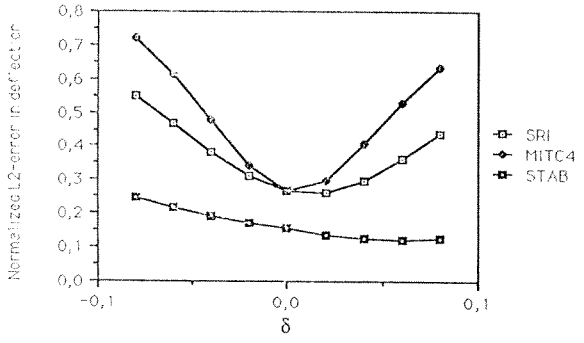

Fig. 9. The distortion sensitivity of the errors $\|w-w_h\|_0/\|w\|_0$ for the 2×2 mesh.

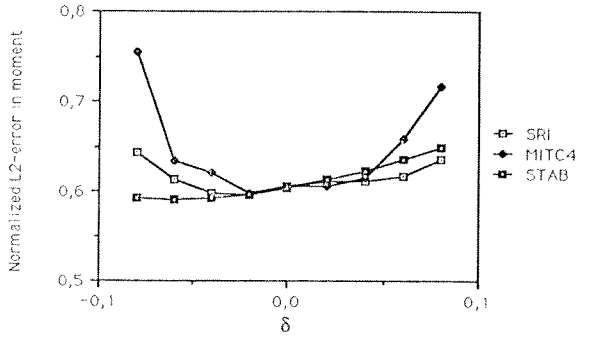

Fig. 10. The distortion sensitivity of the errors $\|\boldsymbol{M}-\boldsymbol{M}_h\|_0/\|\boldsymbol{M}\|_0$ for the 2×2 mesh.

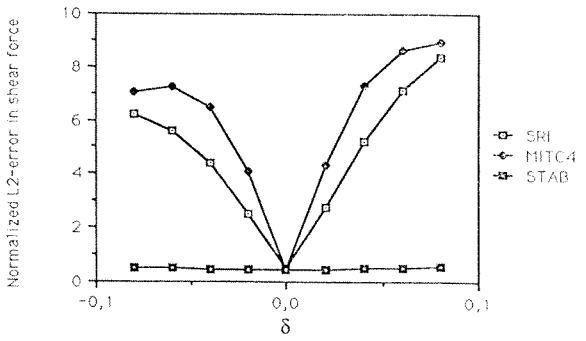

Fig. 11. The distortion sensitivity of the errors $\|Q - Q_h\|_0 / \|Q\|_0$ for the 2×2 mesh.

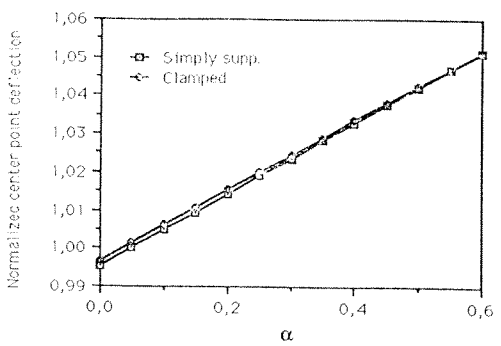

Fig. 12. The dependence of the error w_h(center)/w(center) on the parameter α.

4.4. *The accuracy of the stabilized MITC4 with respect to the parameter* α

In all our previous calculations, we have chosen the parameter α equal to 0.1 (and the mesh length h_K as the length of the longest side of the element K). Here we show the results of some calculations in which we check the accuracy of the method with respect to α. We do the calculations for both a clamped and a simply supported plate. We take the distorted meshes of Fig. 3 with $N = 8$ for the clamped plate and $N = 4$ for the simply supported case (both cases fit into the same pictures).

From the first figure we see that a higher α gives a 'softer' plate. From Fig. 13, we see that the stabilized method gives a smaller L^2-error than the original MITC4 (i.e. the method with $\alpha = 0$) for the whole range $0 < \alpha < 0.2$. For the simply supported plate, this is the case for $0 < \alpha < 0.6$.

The moment is not much influenced by the choice of α as can be seen from Fig. 14.

For the clamped plate, the accuracy of the shear is greatly influenced by the choice of α. For the simply supported case, the influence is smaller. The reason for this is probably that the clamped boundary conditions is the 'worst case' with respect to the stability of the method.

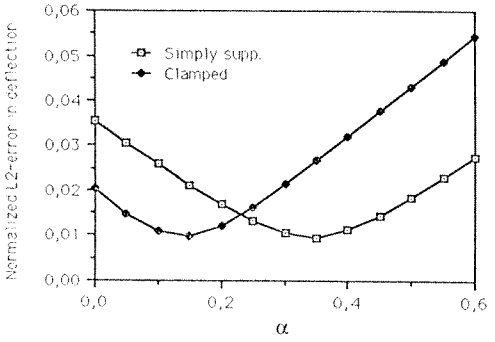

Fig. 13. The dependence of the error $\|w - w_h\|_0 / \|w\|_0$ on the parameter α.

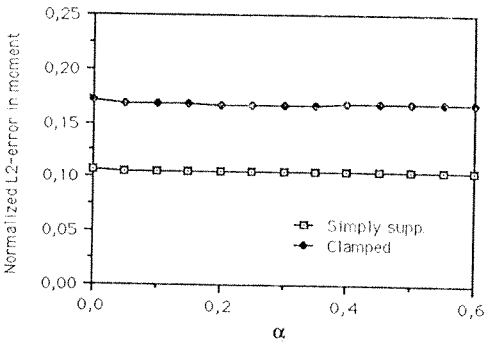

Fig. 14. The dependence of the error $\|M - M_h\|_0 / \|M\|_0$ on the parameter α.

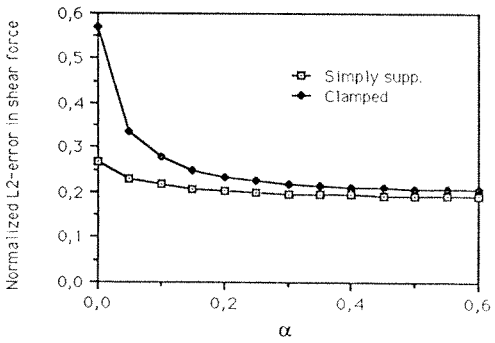

Fig. 15. The dependence of the error $\|Q - Q_h\|_0 / \|Q\|_0$ on the parameter α.

5. Conclusions

In this paper, we have introduced a new stable modification of the MITC4 plate bending element introduced by Bathe and Dvorkin. By performing numerical experiments, we have shown the importance of the stability of a method. In our examples, we considered the original MITC4, the new modification of it and the bilinear element with a reduced one-point integration for the shear term. The examples show that the method with reduced integration is highly unreliable and should not be used. The MITC4 performs much better, but for irregular meshes or very thin plates, it suffers from a decrease in accuracy. Especially the shear force can be oscillating and inaccurate, but the deflection can also be affected. The new modification of the MITC4 does not have these drawbacks; it works well in all calculations performed.

Our numerical examples also show that in order to perform revealing benchmark calculations, it is not enough to do calculations for regular meshes; for those, all three methods perform excellently. Neither is it enough to report on, say, the centerpoint deflection and the moments. Instead all variables of interest should be checked.

Finally, we would like to remark that, in view of the way the shear term is modified in our new element, the 'shear correction factor' does not seem to be a very relevant parameter for the plate model.

References

[1] D.N. Arnold and R.S. Falk, A uniformly accurate finite element method for the Reissner–Mindlin plate, SIAM J. Numer. Anal. 26 (1989) 1276–1290.
[2] D.N. Arnold and R.S. Falk, Edge effects in the Reissner–Mindlin plate theory, in: A.K. Noor, T. Belytschko and J.C. Simo, eds., Analytical and Computational Models of Shells (ASME, New York, 1989) 71–89.
[3] K.J. Bathe and F. Brezzi, On the convergence of a four node plate bending element based on Reissner–Mindlin theory, in: J.R. Whiteman, ed., The Mathematics of Finite Elements and Applications V. MAFELAP 1984 (Academic Press, New York, 1985) 491–503.
[4] K.J. Bathe and F. Brezzi, A simplified analysis of two plate bending elements – The MITC4 and MITC9 elements, in: G.N. Pande and J. Middleton, eds., NUMETA 87, Vol. 1, Numerical Techniques for Engineering Analysis and Design (Martinus Nijhoff, Dordrecht, 1987) D46/1.
[5] K.J. Bathe, F. Brezzi and M. Fortin, Mixed-interpolated elements for Reissner–Mindlin plates. Internat. J. Numer. Methods Engrg. 28 (1989) 1787–1801.
[6] K.J. Bathe and E. Dvorkin, A four node plate bending element based on Mindlin–Reissner plate theory and mixed interpolation, Internat. J. Numer. Methods Engrg. 21 (1985) 367–383.
[7] F. Brezzi and M. Fortin, Numerical approximation of Mindlin–Reissner plates, Math. Comp. 47 (1986) 151–158.
[8] F. Brezzi, M. Fortin and R. Stenberg, Error analysis of mixed-interpolated elements for Reissner–Mindlin plates, Math. Models Methods Appl. Sci. 1 (1991) 125–151.
[9] R.D. Cook, D.S. Malkus and M.E. Plesha, Concepts and Applications of Finite Element Analysis, 3rd Edition (Wiley, New York, 1989).
[10] A.E. Green and W. Zerna, Theoretical Elasticity (Oxford Univ. Press, Oxford, 1968).
[11] T.J.R. Hughes, The Finite Element Method. Linear Static and Dynamic Analysis (Prentice Hall, Englewood Cliffs, NJ, 1987).
[12] T.J.R. Hughes and L.P. Franca, A mixed finite element formulation for Reissner–Mindlin plate theory: Uniform convergence of all higher-order spaces, Comput. Methods Appl. Mech. Engrg. 67 (1988) 223–240.
[13] T.J.R. Hughes and T.E. Tezduyar, Finite elements based upon Mindlin plate theory with particular reference to the four node bilinear isoparametric element, J. Appl. Mech. 48 (1981) 587–598.
[14] L.P. Franca and R. Stenberg, A modification of a low-order Reissner–Mindlin plate bending element, in: J.R. Whiteman, ed., The Mathematics of Finite Elements and Applications VII. MAFELAP 1990 (Academic Press, New York, 1991) 425–436.
[15] C. Johnson and J. Pitkäranta, Analysis of some mixed finite element methods related to reduced integration, Math. Comp. 38 (1982) 375–400.
[16] D. Lasry and T. Belytschko, Transverse shear oscillations in four-node quadrilateral plate elements, Comput. & Structures 27 (1987) 393–398.
[17] R.H. MacNeal, Derivation of element stiffness matrices by assumed strain distribution, Nucl. Engrg. Design 70 (1982) 3–12.
[18] P. Peisker, A multigrid method for Reissner–Mindlin plates, Numer. Math. 59 (1991) 511–528.
[19] J. Pitkäranta, Analysis of some low-order finite element schemes for Mindlin–Reissner and Kirchhoff plates, Numer. Math. 53 (1988) 237–254.

[20] J. Pitkäranta and R. Stenberg, Error bounds for the approximation of Stokes problem with bilinear/constant elements on irregular quadrilateral meshes, in: J.R. Whiteman, ed., The Mathematics of Finite Elements and Applications V. MAFELAP 1984 (Academic Press, New York, 1985) 325–334.
[21] J.G. Simmonds, A Brief on Tensor Analysis (Springer, Berlin, 1982).
[22] R. Stenberg, in preparation.
[23] R. Stenberg and T. Vihinen, On some bilinear elements for Reissner–Mindlin plates, in: R. Glowinski, ed., Proc. 10th Internat. Conf. on Computing Methods in Applied Sciences and Engineering (Nova Science, New York, 1992) 175–183.
[24] S.L. Weissman and R.L. Taylor, Resultant fields for mixed plate bending elements, Comput. Methods Appl. Mech. Engrg. 79 (1990) 321–355.
[25] J.M. Thomas, Thesis, Universite Pierre et Marie Curie, 1977.